Distance-Dependent Beam Split Aided Low-Overhead Near-field Wideband Beam Training

Tianyue Zheng, and Linglong Dai
Department of Electronic Engineering, Tsinghua University,
Beijing National Research Center for Information Science and Technology (BNRist), Beijing 100084, China
Email: zhengty22@mails.tsinghua.edu.cn, daill@tsinghua.edu.cn

2024 IEEE 100th Vehicular Technology Conference (VTC2024-Fall) | 979-8-3315-1778-6/24/$31.00 ©2024 IEEE | DOI: 10.1109/VTC2024-Fall63153.2024.10757929

***Abstract*—In extremely large-scale multiple input multiple output (XL-MIMO) systems for future 6G communications, codebook-based beam training stands out as a promising technology to acquire channel state information. Due to sharp increase in the number of antennas, the transition of electromagnetic propagation from the far-field to the near-field introduces extremely high overhead when employing exhaustive search in both angle and distance domain. To reduce the overwhelming overheads, existing method has been proposed to utilize the dispersed directional beams produced by controllable beam split to simultaneously search multiple directions in a distance ring in wideband communications. However, the method still requires exhaustive search in the distance domain and thus cannot achieve low-overhead beam training for XL-MIMO. To address the problem, achieving a transition from distance-independent beam split to distance-dependent beam split, we propose a near-field beam training method where both different angles and distances can be searched in a pilot simultaneously, and thus a few pilots are capable of covering the whole two-dimensional space for wideband XL-MIMO. Numerical simulations are displayed to verify the performance of the proposed low-overhead method.**

***Index Terms*—Beam training, extremely large-scale MIMO (XL-MIMO), near-field, wideband.**

I. Introduction

The extremely large-scale MIMO (XL-MIMO) is a promising technique for 6G [1]. Thanks to the significantly large number of antennas, the spatial multiplexing gain and beamforming gain could be significantly enhanced in XL-MIMO. To harvest these benefits of XL-MIMO, beam training becomes essential to assign the directional beams to users, which is realized by transmitting predefined directional beams (codewords), and selecting the optimal codeword according to the user's received powers [2].

Compared with 5G massive MIMO, beam training for 6G XL-MIMO will induce overwhelming training overheads due to the fundamental change in electromagnetic (EM) field property. Specifically, in 5G when antenna number is not very large, channel model mainly considers far-field propagation where radiated EM waves can be approximated as planar waves. Then the array response vector of channel is only associated with the angle and orthogonal Discrete Fourier Transform (DFT) codebook can be utilized in far-field beam training to perform efficient scanning in the angle domain [3].

With the transition from massive MIMO to XL-MIMO, the increased array aperture leads to more users located in spherical-wave-based near-field regions [4]. The array response vector of the near-field channel is not only associated with the angle but also with the distance. Therefore, to perform near-field beam training, the polar-domain codebook is proposed in [4] to scan both angle and distance domain. It may result in unacceptable pilot overheads for near-field beam training since it involves two-dimension exhaustive search for all possible beam directions and distances.

To cope with this problem, both narrowband and wideband methods have been proposed. Narrowband methods attempt to reduce the beam training overheads with hierarchical beam training [5], inference from far-field beam training [6], and combinations of above methods [7]. The methods can to some extent reduce the training overheads, but they only measure the received power of one subcarrier in a single time slot, which limits the efficiency of near-field beam training. It motivates us to develop wideband XL-MIMO beam training methods, which utilize information in multiple subcarriers to further reduce the beam training overheads. Unfortunately, few works have been focused on wideband XL-MIMO beam training.

Excavating frequency resources, in [8] we have proposed a wideband beam training scheme, namely near-field rainbow, based on controllable beam split. By setting the time-delay parameters, multiple beams at different frequencies are focused on multiple angles in a specific distance ring. Thus, multiple angles can be searched in a single time slot, which may significantly improve the beam training efficiency. However, since the beam split in [8] is essentially distance-independent beam split, it does not well match angle-distance instincts of near field channel. Thus, the optimal distance is obtained by sequentially testing different distance rings, which could not fully unleash the capability of beam-split.

To tackle this problem, this paper attempts to exploit the *distance-dependent* feature of near-field beam-split. We propose a near-field beamforming method to distribute multi-frequency-beams on multiple angle-and-distances simultaneously in one time-slot, achieving low-overhead beam training. Specifically, we first reveal the mechanism of controllable distance-dependent beam split. The cooperative manipulation of time delay and phase shift of beamformer can spread the focal points of multi-frequency-beams on different angles of *multi-distance-rings*. Then, using the mechanism of distance-dependent beam split, a wideband beam training method is proposed. In the scheme, both angle and distance domain can be searched with beams of different subcarriers in a single pilot. Finally, we provide simulation results to verify the performance of proposed beam training scheme.

II. System Model

In this section, we first introduce the near-field wideband channel model in XL-MIMO systems and formulate the near-field beam training problem. Then, we will briefly review the existing controllable near-field beam split proposed in [8].

A. Near-Field Wideband Channel Model

In this paper, a wideband THz XL-MIMO system is considered. The BS equipped with an $N_t = 2N+1$-antenna uniform linear array serves a single-antenna user using orthogonal frequency division multiplexing (OFDM) of M subcarriers. The bandwidth, central carrier frequency, central wavelength, and antenna spacing are denoted as B, f_c, λ_c, and $d = \lambda_c/2$. Consider the downlink transmission. Let $s_m \in \mathbb{C}$ be the normalized transmitted symbol at f_m, then the received signal y_m at the UE of the m-th subcarrier is given by

$$y_m = \sqrt{P_t}\boldsymbol{h}_m^H \boldsymbol{w}_m s_m + n_m, \tag{1}$$

where $P_t > 0$ is the transmit power, $\boldsymbol{h}_m$ the downlink channel, $\boldsymbol{w}_m$ the unit-norm beamformer, and n_m the complex circularly-symmetric Gaussian noise $n_m \sim \mathcal{CN}(0, \sigma^2)$ at the UE receiver with variance σ^2.

Due to the severe path loss incurred by the scatters, THz communications heavily rely on the line-of-sight (LoS) path [9]. Therefore, using Saleh-Valenzuela channel model [10], the downlink channel $\mathbf{h}_m \in \mathbb{C}^{N_t \times 1}$ at the m-th subcarrier can be denoted as

$$\mathbf{h}_m = \sqrt{N_t}\beta_m e^{-j2\pi k_m r}\mathbf{a}_m(\theta, r), \tag{2}$$

where f_m denotes the frequency of the m-th subcarrier satisfying $f_m = fc + \frac{B}{M}(m - 1 - \frac{M-1}{2})$ and β_m, $k_m = 2\pi f_m/c$, $\theta = \sin\vartheta$, r denote the path gain of f_m, wavenumber of f_m, spatial direction and distance from the UE to the center of the antenna array. The path gain β_m can be modeled as

$$\beta_m = \frac{\lambda_m}{4\pi r} = \frac{f_m}{f_c}\beta_c, \tag{3}$$

where β_c is the path gain at central frequency f_c.

The near-field array response vector $\mathbf{a}_m(\theta, r)$ in (2) is derived on the basis of spherical wave assumption:

$$\mathbf{a}_m(\theta, r) = \frac{1}{\sqrt{N_t}}[e^{-jk_m(r^{(-N)}-r)}, \ldots, e^{-jk_m(r^{(N)}-r)}]^T \tag{4}$$

where $r^{(n)} = \sqrt{r^2 + n^2d^2 - 2r\theta nd}$ denotes the distance from the n-th transmitter antenna to the UE. For fixed $\alpha = \frac{1-\theta^2}{2r}$, the curve plotted by (r, θ) is viewed as to a distance ring in the physical space. By Taylor expansion, $\mathbf{a}_m(\theta, r)$ can be approximated with $\mathbf{b}_m(\theta, \alpha)$ written as

$$[\mathbf{b}_m(\theta, \alpha)]_n = \frac{1}{\sqrt{N_t}}e^{jk_m(nd\theta - n^2d^2\alpha)}. \tag{5}$$

Since $\sqrt{N_t}\beta_m e^{-j2\pi k_m r}$ in (2) is independent of the antenna index n, we only need to discuss the vector $\mathbf{b}_m(\theta, \alpha)$.

B. Formulation of Near-Field Beam Training Problem

The near-field beam training desires to obtain the location information (θ, α) of the dominant path between the BS and the user and align the beamforming vector with this location. The optimal beamforming vector is selected from a predefined polar-domain codebook [4], which can be represented as

$$\mathcal{A}_m = [\mathbf{b}_m(\theta_1, \alpha_1^1), \cdots, \mathbf{b}_m(\theta_1, \alpha_1^{S_1}), \cdots, \mathbf{b}_m(\theta_{N_t}, \alpha_1^{S_{N_t}})], \tag{6}$$

where each column of polar-domain codebook $\mathcal{A}_m$ is a codeword aligned with the grid $(\theta_n, \alpha_n^{s_n})$, with $s_n = 1, 2, \cdots, S_n$, and S_n denotes the number of sampled distance grids at θ_n. When conducting exhaustive search, we sequentially employ the codewords to perform beamforming and select the codeword corresponding to the largest received power to obtain the estimated physical location $(\hat{\theta}, \hat{\alpha})$, i.e.

$$(\hat{\theta}, \hat{\alpha}) = \arg\max_{\theta,\alpha} \sum_{m=1}^{M} \|y_m\|^2. \tag{7}$$

Finally, a near-field beam $\boldsymbol{w}_m = \mathbf{b}_m(\hat{\theta}, \hat{\alpha})$ aligned with the location $(\hat{\theta}, \hat{\alpha})$ can be obtained to serve the user. Thus, the size of the polar-domain codebook is the product of the antenna number at BS and the number of sampled distance grids, leading to unaffordable beam training overheads.

C. Controllable Near-Field Distance-Independent Beam split

In this subsection, we will review the mechanism of controllable near-field beam split proposed in [8] and explain how to employ it to achieve efficient beam training. We utilize a fully-connected time delay (TD)- phase shift (PS) precoding structure where each antenna is sequentially connected to a time delay unit and a phase shift unit. A TD unit is capable of tuning *frequency-dependent* phase shift by adjusting the time delay. We denote the TD beamforming vector with normalized power constraint at m-th subcarrier as $\mathbf{w}_m^{\mathrm{TD}}$

$$[\mathbf{w}_m^{\mathrm{TD}}]_n = \frac{1}{\sqrt{N_t}}e^{-j2\pi f_m \tau^{(n)'}} = \frac{1}{\sqrt{N_t}}e^{-jk_m r_1^{(n)'}} \tag{8}$$

where $\tau^{(n)'}$ is the adjustable delay of the n-th TD unit, while $r_1^{(n)'} = c\tau^{(n)'}$. We use the superscript $'$ to indicate the adjustable parameters. Since $\mathbf{w}_m^{\mathrm{TD}}$ has a similar form to the array response vector $\mathbf{b}_m(\theta, \alpha)$, we can set $r_1^{(n)'}$ as $r_1^{(n)'} = nd\theta_1' - n^2d^2\alpha_1'$, where θ_1', α_1' are defined as the adjustable TD parameters. Accordingly, the beamforming vector at f_m can be presented as

$$[\mathbf{w}_m^{\mathrm{TD}}(\theta_1', \alpha_1')]_n = \frac{1}{\sqrt{N_t}}e^{-jk_m(nd\theta_1' - n^2d^2\alpha_1')}. \tag{9}$$

Furthermore, the beamforming vector generated by *frequency-independent* phase shift $\mathbf{w}^{\mathrm{PS}}$ is denoted as

$$\mathbf{w}^{\mathrm{PS}} = \frac{1}{\sqrt{N_t}}[e^{-jk_c r_2^{(-N)'}}, \ldots, e^{-jk_c r_2^{(N)'}}], \tag{10}$$

where $r_2^{(n)'}$ is the n-th adjustable PS parameter. Similarly, the n-th element of $\mathbf{w}_m^{\mathrm{PS}}$ is set as

$$[\mathbf{w}^{\mathrm{PS}}(\theta_2', \alpha_2')]_n = \frac{1}{\sqrt{N_t}}e^{-jk_c(nd\theta_2' - n^2d^2\alpha_2')}. \tag{11}$$

where θ_2', α_2' are correspondingly adjustable PS parameters.

Configuring TD-PS precoding structure with θ_1',α_1',θ_2' and α_2', the array gain at the m-th subcarrier on an arbitrary location (θ, α) can be presented as

$$\begin{aligned} & |(\mathbf{w}_m^{\mathrm{TD}}(\theta_1', \alpha_1') \odot \mathbf{w}^{\mathrm{PS}}(\theta_2', \alpha_2'))^T \mathbf{b}_m(\theta, \alpha)| \\ = & \frac{1}{N_t} \left| \sum_{n=-N}^{N} e^{jnd(k_m\theta - k_m\theta_1' - k_c\theta_2') - jn^2d^2(k_m\alpha - k_m\alpha_1' - k_c\alpha_2')} \right| \\ = & G(k_m\theta - k_m\theta_1' - k_c\theta_2', k_m\alpha - k_m\alpha_1' - k_c\alpha_2'), \end{aligned} \tag{12}$$

where we define $G(x, y) = 1/N_t \left| \sum_{n=-N}^{N} e^{jndx - jn^2d^2y} \right|$ and it achieves a maximal solution at $(x, y) = (0, 0)$ [4]. According to [8], the beam at frequency f_m is focused on the location (θ_m, α_m) with the maximum array gain, and thereby we obtain $k_m\theta - k_m\theta_1' - k_c\theta_2' = 0$ and $k_m\alpha - k_m\alpha_1' - k_c\alpha_2' = 0$. Thus, the beam at frequency f_m aligns with the location:

$$\theta_m = \theta_1' + \frac{f_c}{f_m}\theta_2', \tag{13}$$

$$\alpha_m = \alpha_1' + \frac{f_c}{f_m}\alpha_2'. \tag{14}$$

By setting $\alpha_2' = 0$ and $\theta_2' \neq 0$, the beams at different frequencies will linearly split towards different spatial angles in the same distance ring. However, it is essentially distance-independent beam split, where beams can cover multiple angles in only *one* specific distance ring. It does not well match angle-distance instincts of near field channel, which still requires exhaustive search in distance domain and limits its efficiency during beam training. To deal with this problem, we will introduce the distance-dependent beam split phenomena and how we can search multiple angles and distances at the same time by utilizing this phenomenon.

III. Distance-Dependent Beam Split and Proposed Near-Field Beam Training Scheme

In this section, the mechanism of distance-dependent beam split will be introduced. By elaborately designing the TD-PS parameters, we can divide the subcarriers over the entire bandwidth into several groups, and beams of each group cover the angular range with different distance ranges. Taking advantage of this mechanism, we propose a distance-dependent beam-split aided near-field beam training method. In the proposed method, multiple distance rings can be covered by the beams at different frequencies simultaneously in the near field and thus both angle and distance dimension can be searched simultaneously with different subcarriers in a single pilot.

A. Controllable Distance-Dependent Beam Split

To illustrate the phenomena, we first analyze the periodicity of the array gain with the TD-PS precoding structure. As proven in [8], $G(x, y)$ is periodic against the vector variable (x, y) with a period of $(\frac{2\pi}{d}, \frac{2\pi}{d^2})$, i.e., $G(x - \frac{2\pi p}{d}, y - \frac{2\pi q}{d^2}) = G(x, y)$, for $\forall p, q \in \mathbb{Z}$. The periodicity implies that $(x, y) = (\frac{2\pi p}{d}, \frac{2\pi q}{d^2})$ are all optimal solutions to maximize the array gain $G(x, y)$. Then we obtain $k_m\theta - k_m\theta_1' - k_c\theta_2' = \frac{2\pi p_m}{d}$ and $k_m\alpha - k_m\alpha_1' - k_c\alpha_2' = \frac{2\pi q_m}{d^2}$ and the focused location (θ_m, α_m) of the beam at frequency f_m is written as

$$\theta_m = \theta_1' + \frac{f_c}{f_m}(\theta_2' + 2p_m), \tag{15}$$

$$\alpha_m = \alpha_1' + \frac{f_c}{f_m}(\alpha_2' + \frac{2q_m}{d}). \tag{16}$$

Since θ_m and α_m correspond to an actual physical angle and distance ring, they are constrained by $\theta_m \in [-1, 1]$ and $\alpha_m > 0$. However, as long as the delay circuits allow, the parameters can be arbitrarily adjusted, making it possible to break the constraint $\theta_1' + \frac{f_c}{f_m}\theta_2' \in [-1, 1]$ and $\alpha_1' + \frac{f_c}{f_m}\alpha_2' > 0$. In this context, the integer p_m and q_m will naturally become non-zero to shift the value of θ_m and α_m into the range.

Then, we illustrate the mechanism of distance-dependent beam split. To begin with, in the angle domain, we adjust the parameters θ_1' and θ_2' such that the beam of the first subcarrier is steered to $\theta_1 = \theta_1' + \frac{f_c}{f_1}\theta_2' = -1$ with $p_1 = 0$. Without loss of generality, we assume $\theta_1' > 0$ and $\theta_2' < 0$. In this case, as the subcarrier frequency f_m grows, the focused direction θ_m gradually increases from -1 to 1 with p_m remaining to 0. Suppose that the value of θ_2' is large enough such that the focused direction θ_m can approach $\theta_{m_1} = \theta_1' + \frac{f_c}{f_{m_1}}\theta_2' = 1$ at the m_1-th subcarrier where $m_1 < M$. Subsequently, if we continue to increase the frequency, then θ_{m_1+1} definitely exceeds 1. Accordingly, the integer p_{m_1+1} will automatically become -1 for guaranteeing the angle constraint $\theta_{m_1+1} = \theta_1' + \frac{f_c}{f_{m_1+1}}(\theta_2' - 2) \in [-1, 1]$. Besides, the beam at frequency f_{m_1+1} is steered to $\theta_1' + \frac{f_c}{f_{m_1+1}}(\theta_2' - 2) \approx -1$. That is to say, due to the periodic property of the angle domain, the spatial direction of beam "skips" from 1 to -1 when the frequency arises from f_{m_1} to f_{m_1+1}. With the continuous increment of the frequency, the focused direction of the beam will gradually rise again and the process will repeat until the last subcarrier f_M. An important insight is that several beams of different frequencies f may focus in the same physical direction. In other words, the beams over the entire bandwidth can periodically scan the angle range $[-1, 1]$.

The major difference between the beam split pattern over the angular and distance dimensions is attributed to the physical constraints imposed on θ_m and α_m. As mentioned earlier, the physical direction θ_m is bounded between -1 and 1 while the distance ring, α_m, can grow from 0 to infinity. Thus, as opposed to the periodic pattern of the angle domain, the focused distance ring α_m increases/decreases monotonically with the frequency f_m, as long as $\alpha_1' + \frac{f_c}{f_m}(\alpha_2' + \frac{2q}{d}) \geq 0$ and $\alpha_2' + \frac{2q}{d} \neq 0$. And during the process, $q_m, m \in \{1, 2, \cdots, M\}$ remains the same, and thus we just ignore the subscript m. For example, if the multi-frequency beams are desired to cover the entire distance range $[\alpha_p, \alpha_q]$, we can simply set

$$\alpha_L = \alpha_1' + \frac{f_c}{f_L}(\alpha_2' + \frac{2q}{d}) \geqslant \alpha_p \tag{17}$$

$$\alpha_H = \alpha_1' + \frac{f_c}{f_H}(\alpha_2' + \frac{2q}{d}) \leqslant \alpha_q, \tag{18}$$

where f_L and f_H are lower and upper subcarrier frequencies.

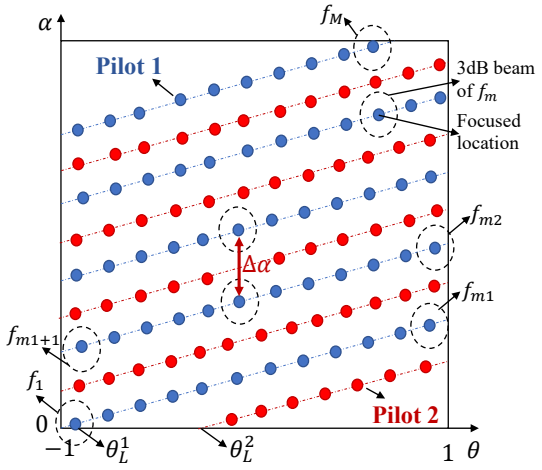

Fig. 1. Beams of different subcarriers in distance-dependent beam split.

In summary, by integrating periodic pattern and monotonous pattern of the angle-dimension and distance-dimension beam splits, we arrive at the distance-dependent beam split effect. As presented in Fig. 1, the focused direction of the multi-frequency beams fluctuate periodically between $[-1, 1]$ while the focused distance ring increases monotonically with the frequency f_m. In such cases, the focused locations $(\theta_m, \alpha_m), m = 1, 2 \dots M$ are distributed over several inclined strips. Each strip covers the entire angle range $[-1, 1]$ while different strips occupy different distance ranges.

B. Distance-Dependent Beam Split based Beam Training

The discovered distance-dependent beam split phenomenon motivates us to design a new near-field beam training method. Firstly, we introduce the basic principles of the method. To support **reliable** beam training, each location inside the communication region must be covered by one training beam. To quantify this metric, we require that each location lies in the 3 dB-beam width of a certain beam. Besides, we aim to utilize as few pilots as possible to improve the **efficiency**.

Building on the above principles, we elaborate on the manipulation of TD-PS parameters. To begin with, let's consider the angle-related parameters θ_2', as well as the integer p. Based on (15), the focused direction difference of adjacent subcarriers on the same strip with $p_m = p_{m+1} = p$ is

$$|\theta_{m+1} - \theta_m| = |f_c(\theta_2' + 2p)(\frac{1}{f_{m+1}} - \frac{1}{f_m})|. \tag{19}$$

On the one hand, (19) suggests that a larger $|\theta_2' + 2p|$ leads to a faster change in the focal angle of beams versus frequency f_m. Thus, a relatively large $|\theta_2' + 2p|$ improves the efficiency of coverage of angle domain. On the other hand, since the direction difference grows linearly with $|\theta_2' + 2p|$, excessively large $\theta_2' + 2p$ will lead to uncovered angular range and the following **Lemma 1** gives the upper bound of $\theta_2' + 2p$ to guarantee the entire coverage.

Lemma 1 *Consider an arbitrary physical location $(\bar{\theta}, \bar{\alpha})$ inside the trajectory scanned by $\{\theta_m, \alpha_m\}$. If $\theta_2' + 2p_m > 0$, to make the direction $\bar{\theta}$ lie in the angle-domain* 3 dB*-beamwidth of a certain beam, the parameter θ_2' should satisfy*

$$\theta_2' \in \left\{\theta_2' : \theta_2' + 2p_m \leqslant \frac{1}{N_t}(f_m + f_{m+1})\frac{M}{B}, \forall p_m \in \mathbb{Z}\right\}. \tag{20}$$

Proof: To guarantee the entire coverage in angle domain, the angle difference of θ_m and θ_{m+1} should be smaller than the sum of the 3 dB-beam width of the beam at the m-th and $m+1$-th subcarrier, which can be denoted as

$$|\theta_{m+1} - \theta_m| \leqslant \eta_\theta^{f_m} + \eta_\theta^{f_{m+1}} \leqslant \frac{1}{N_t}(\frac{f_c}{f_{m+1}} + \frac{f_c}{f_m}), \tag{21}$$

where η_θ^f is the 3 dB-beam width of the beam in the angle domain for frequency f. Combining (19) and (21) gives rise to the results of (20) in **Lemma 1**. ■

It is obvious that for distance-dependent beam split, p_m increases with frequency f_m, and thus by setting

$$\theta_2' \in \left\{\theta_2' : \theta_2' + 2p_M \leqslant \frac{2f_L M}{N_t B}, \forall p_M \in \mathbb{Z}\right\}, \tag{22}$$

(20) holds for all subcarriers.

Next, we continue to discuss the manipulation of distance-related parameters α_1', α_2' and q. If the possible user distribution distance is with $[\alpha_{\min}, \alpha_{\max}]$, by setting $\alpha_p = \alpha_{\min}$ and $\alpha_q = \alpha_{\max}$, $\alpha_2' + \frac{2q}{d}$ is supposed to satisfy

$$\alpha_2' \in \left\{\alpha_2 : \alpha_2' + \frac{2q}{d} \leqslant \frac{\alpha_{\max} - \alpha_{\min}}{\frac{f_c}{f_L} - \frac{f_c}{f_H}}, \forall q \in \mathbb{Z}\right\}. \tag{23}$$

After obtaining $\alpha_2' + \frac{2q}{d}$, the parameter α_1' is manipulated as $\alpha_1' \in [\alpha_{\max} - \frac{f_c}{f_L}(\alpha_2' + \frac{2q}{d}), \alpha_{\min} - \frac{f_c}{f_H}(\alpha_2' + \frac{2q}{d})]$.

As shown in Fig. 1, for a particular angle the distance difference of the adjacent searched location is defined as $\Delta\alpha$. Based on Taylor expansion, (15)-(16) suggest that the angle and distance difference of these two locations is

$$\Delta\theta = \frac{\theta_2' + 2p}{f_c}\Delta f = 2, \tag{24}$$

$$\Delta\alpha = \frac{\alpha_2' + \frac{2q}{d}}{f_c}\Delta f, \tag{25}$$

where $\Delta\theta$, Δf are the angle difference and frequency difference. Then the distance difference $\Delta\alpha$ can be written as

$$\Delta\alpha = \frac{2(\alpha_2' + \frac{2q}{d})}{\theta_2' + 2p}. \tag{26}$$

Similar to (21), the distance difference $\Delta\alpha$ should be smaller than the sum of the 3 dB-beam width of the beam in the distance domain, which can be presented as

$$\Delta\alpha \leqslant \eta_\alpha^{f_a} + \eta_\alpha^{f_b}, \tag{27}$$

where f_a and f_b is the frequency of the a-th and b-th subcarrier and η_α^f is the 3 dB-beam width in the distance domain.

However, in practice, (27) may not be satisfied which means a single pilot cannot search the entire region. Thus, in addition to the guarantee of angular coverage by manipulation of angle-

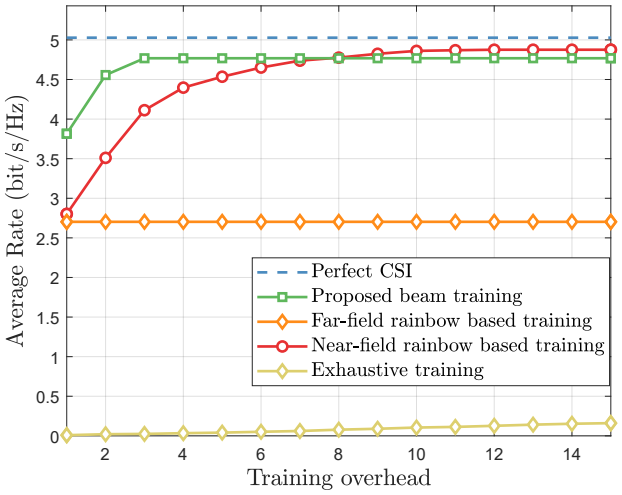

Fig. 2. Average rate performance vs. training overhead.

related parameters, we utilize interleaved pilots to guarantee the entire coverage in the distance domain. For each pilot, θ_2', α_1' and α_2' remain the same while θ_1' is set as different values to adjust the starting direction θ_L. Then we will illustrate the number of pilots required and the corresponding manipulation of θ_1'. 3 dB-beam width in distance domain can be numerically calculated as [4]

$$\beta = \sqrt{\frac{N_t^2 d^2 (1-\theta^2)}{2\lambda}\left(\frac{1}{r}-\frac{1}{\bar{r}}\right)} \approx 1.557. \tag{28}$$

Thus, we obtain

$$|\alpha - \bar{\alpha}| = \frac{\beta^2 \lambda}{N_t^2 d^2} \leqslant \frac{4\beta^2 f_c^2}{N_t^2 c f_H}. \tag{29}$$

Therefore, the minimal pilot number required is calculated as

$$K \geqslant \frac{\Delta\alpha}{|\alpha - \bar{\alpha}|} \geqslant \frac{(\alpha_2' + \frac{2q}{d}) N_t^2 c f_H}{2(\theta_2' + 2p)\beta^2 f_c^2}. \tag{30}$$

Obtaining the pilot number K, we adjust θ_1' to make θ_L of K randomly distributed within $[-1, 1]$ as $\theta_L^1, \theta_L^2, \cdots, \theta_L^K$ by

$$\theta_1'^k + 2(\theta_2' + 2p) = \theta_L^k. \tag{31}$$

During beam training, BS sequentially transmits K pilots to the user. The user selects the subcarrier with the highest received power and estimates physical location with (15)-(16).

IV. Simulation Results

We consider a wideband XL-MIMO system, where the BS equips an $N_t = 256$-element ULA with TD-PS beamforming architecture. The carrier frequency is $f_c = 30$ GHz, the number of sub-carriers is $M = 1024$, and the bandwidth is $B = 3$ GHz. The users are uniformly distributed within angle range $[-\pi/3, \pi/3]$, and the potential distance ring $[\alpha_{\min}, \alpha_{\max}] = [1/400, 1/10]$. We use the average rate performance to quantify the beam training performance.

We compare the proposed method with several benchmarks. In Fig. 2, we illustrate the average rate performance against the training overhead. The SNR is set as 15 dB. In each time slot, we utilize the optimal beamforming vector we have searched in previous time slots to serve the user. The far-field beam split-based technique only needs one pilot. However, since the far-field approach only considers the angle information while ignoring the distance information, their average rate performance is not satisfactory. Besides, the near-field exhaustive scheme performs extremely badly with low overheads. Then we focus on the comparison of near-field beam split-based beam training [8] and the proposed method. As depicted in Fig. 2, the proposed method employs only 3 pilots to achieve comparable average rate performance while near field beam split-based method [8] requires 10 (equal to the number of samples distance). Since both the angle and distance domain can be searched with different subcarriers simultaneously, the proposed method further improves the beam training efficiency to achieve low-overhead XL-MIMO beam training.

V. Conclusions

In this paper, we demonstrate a phenomena called distance-dependent beam split where we can divide the subcarriers into different groups which periodically cover the angular range with different distance ranges by elaborately manipulation of the TD-PS parameters. Then a wideband beam training method has been proposed based on the new discovery, where both angle and distance domain can be searched with beams of different subcarriers in a single pilot. Simulation results have verified the effectiveness of the proposed method, which serves as a promising way to achieve low-overhead beam training for XL-MIMO. Future works can be focused on extending the work to uniform planar arrays.

References

[1] E. D. Carvalho, A. Ali, A. Amiri, M. Angjelichinoski, and R. W. Heath, "Non-stationarities in extra-large-scale massive MIMO," *IEEE Wireless Commun.*, vol. 27, no. 4, pp. 74–80, Aug. 2020.

[2] W. Liu, C. Pan, H. Ren, F. Shu, S. Jin, and J. Wang, "Low-overhead beam training scheme for extremely large-scale RIS in near field," *IEEE Trans. Commun.*, vol. 71, no. 8, pp. 4924–4940, Aug. 2023.

[3] A. Alkhateeb, G. Leus, and R. W. Heath, "Limited feedback hybrid precoding for multi-user millimeter wave systems," *IEEE Trans. Wireless Commun.*, vol. 14, no. 11, pp. 6481–6494, Nov. 2015.

[4] M. Cui and L. Dai, "Channel estimation for extremely large-scale MIMO: Far-field or near-field?" *IEEE Trans. Commun.*, vol. 70, no. 4, pp. 2663–2677, Apr. 2022.

[5] Y. Lu, Z. Zhang, and L. Dai, "Hierarchical beam training for extremely large-scale MIMO: From far-field to near-field," *IEEE Trans. Commun,*, 2023.

[6] Y. Zhang, X. Wu, and C. You, "Fast near-field beam training for extremely large-scale array," *IEEE Wireless Commun. Lett.*, vol. 11, no. 12, pp. 2625–2629, Dec. 2022.

[7] W. Liu, H. Ren, C. Pan, and J. Wang, "Deep learning based beam training for extremely large-scale massive MIMO in near-field domain," *IEEE Commun. Lett.*, vol. 27, no. 1, pp. 170–174, Jan. 2023.

[8] M. Cui, L. Dai, Z. Wang, S. Zhou, and N. Ge, "Near-field rainbow: Wideband beam training for xl-mimo," *IEEE Trans. Wireless Commun.*, vol. 22, no. 6, pp. 3899–3912, Jun. 2023.

[9] H. Elayan, O. Amin, B. Shihada, R. M. Shubair, and M.-S. Alouini, "Terahertz band: The last piece of rf spectrum puzzle for communication systems," *IEEE Open J. Commun. Soc.*, vol. 1, pp. 1–32, 2020.

[10] A. Alkhateeb, O. El Ayach, G. Leus, and R. W. Heath, "Channel estimation and hybrid precoding for millimeter wave cellular systems," *IEEE J. Sel. Top. Signal Process.*, vol. 8, no. 5, pp. 831–846, Oct. 2014.